

# Virtual Cisternoscopy: 3D MRI Models of the Cerebellopontine Angle for Lesions Related to the Cranial Nerves

James D. Rabinov, M.D.,<sup>1</sup> Frederick G. Barker, M.D.,<sup>2</sup> Michael J. McKenna, M.D.,<sup>3</sup> and Hugh D. Curtin, M.D.<sup>4</sup>

## ABSTRACT

---

This study was conducted to show that high-resolution magnetic resonance imaging (MRI) can aid in the neurosurgical approach to lesions affecting the cranial nerves (CNs) in the cerebellopontine angle (CPA). Three patients with symptomatology related to CNs VII and VIII underwent MRI examinations performed on a 1.5-Tesla Siemens MR scanner. As part of these routine examinations, the imaging technique of constructive interference in the steady state (CISS) was used to collect a volume of data through the brainstem and internal auditory canals. This high-resolution technique acquires a three-dimensional (3D) volume of data at 0.7-mm intervals. Parameters included TR 12.3/TE 5.9, number of acquisitions of 2, a matrix of  $230 \times 512$ , bandwidth of 130 Hz per pixel, and time of 8:40. Data were transferred to a commercially available GE workstation and reconstructed into a 3D surface-rendered model. This interactive method allows the model to be visualized from any angle, including that of a standard skull base approach of suboccipital craniotomy for access to the CPA cistern. The images shown include the CPA cistern as seen from the suboccipital surgical approach. CNs V, VII, and VIII can easily be seen in relation to the pons and petrous face. The relationship between the CNs and acoustic neuromas and skull base tumors can be evaluated. Vascular structures, which are often seen in relation to CNs VII and VIII, can be viewed in a 3D format to determine the need for microvascular decompression. Direct intraoperative photographs taken through the operating microscope confirmed the anatomic accuracy of the 3D models. Imaging used for interactive neurosurgical planning must demonstrate a high degree of anatomic detail. Virtual cisternoscopy using CISS MRI technique can achieve the required resolution. Reconstruction algorithms to create surface rendering can generate

---

*Skull Base*, volume 14, number 2, 2004. Address for correspondence and reprint requests: James D. Rabinov, M.D., Neuroradiology/Gray 289, Massachusetts General Hospital, 55 Fruit St., Boston, MA 02114. E-mail: jrabinov@partners.org. Massachusetts General Hospital, Departments of <sup>1</sup>Neuroradiology and <sup>2</sup>Neurosurgery, Boston, Massachusetts; and Massachusetts Eye and Ear Infirmary, Departments of <sup>3</sup>Otolaryngology and <sup>4</sup>Radiology, Boston, Massachusetts. Copyright © 2004 by Thieme Medical Publishers, Inc., 333 Seventh Avenue, New York, NY 10001, USA. Tel: +1(212) 584-4662. 1531-5010,p;2004,14,02,093,99,ftx,en;sbs00389x.

images with similar 3D anatomic detail to that seen during neurosurgical approaches to the CPA cistern.

**KEYWORDS:** 3D MRI model, acoustic neuroma, CISS

Three-dimensional (3D) computer-generated models can be created from anatomic magnetic resonance imaging (MRI) data.<sup>1,2,3</sup> These models can be viewed in a navigational mode to provide presurgical planning such as virtual endoscopy of the inner ear in patients considered for cochlear implant.<sup>4,5</sup> It has been used to examine the cisternal segments of cranial nerves (CNs) in normal patients and patients with suspected neural compression syndrome from adjacent vasculature.<sup>3,6</sup> The purpose of this study is to show that high-resolution 3D models based on MRI data can produce an interactive model to aid in planning the neurosurgical approach to vascular and neoplastic lesions affecting the CNs in the cerebellopontine angle (CPA).

## METHODS AND MATERIALS

Three patients with symptomatology related to CNs VII and VIII underwent MRI examinations performed with a standard 1.5-Tesla Siemens MR scanner. Constructive interference in the steady state (CISS) was used to collect a volume of data through the brainstem and internal auditory canals (IACs). Parameters include TR (repetition time), 12.3 millisecond; TE (echo time), 5.9 millisecond; AC (number of acquisitions), 2; matrix, 230 × 512; bandwidth, 130 Hz per pixel; and time, 8:40. This high-resolution technique acquires a 3D volume of data at 0.7-mm slice thickness. The sequence produces images with a heavily T2-weighted appearance. Fluid such as cerebrospinal fluid (CSF) and endolymph are bright while soft tissue structures including the brainstem, CNs, blood vessels as well as bony structures of the skull base have a

similar low-signal intensity. Soft tissue tumors appear similar to their appearance on T2-weighted imaging.

Data were transferred to a commercially available GE workstation (4.1 software) and reconstructed into a 3D surface-rendered model. The "CISS data" was selected and processed under "Volume Analysis" followed by "Head Protocol" and then "Navigator Circle of Willis." The "v" located in the upper left of the navigator image was switched to "white in black," and the threshold was set to 200 and the aperture to 100. The data could then be viewed from any vantage point in the CSF space while the reference point on the planar images was moved on the navigator screen. Standard 2D reformat images could also be reconstructed in any plane to follow a particular structure of interest, for example, images orthogonal to the axis of the IAC to follow CNs VII and VIII.

## RESULTS

The 3D datasets were reconstructed to produce an interactive surface model that could be viewed from any angle or point in the CSF space. This interactive mode can be used to zoom in or out and to follow the CNs and vessels in relation to CPA lesions. The inferior-to-superior view provided a view similar to that a neurosurgeon might see during a suboccipital craniotomy to access the CPA cistern. Figures 1A to 1D demonstrate CNs V, VII, and VIII in relation to the pons and petrous face using 2D reformats and images from the 3D navigational program. These surface-rendered images show that the CPA cistern can also be viewed from the suboccipital approach. Direct

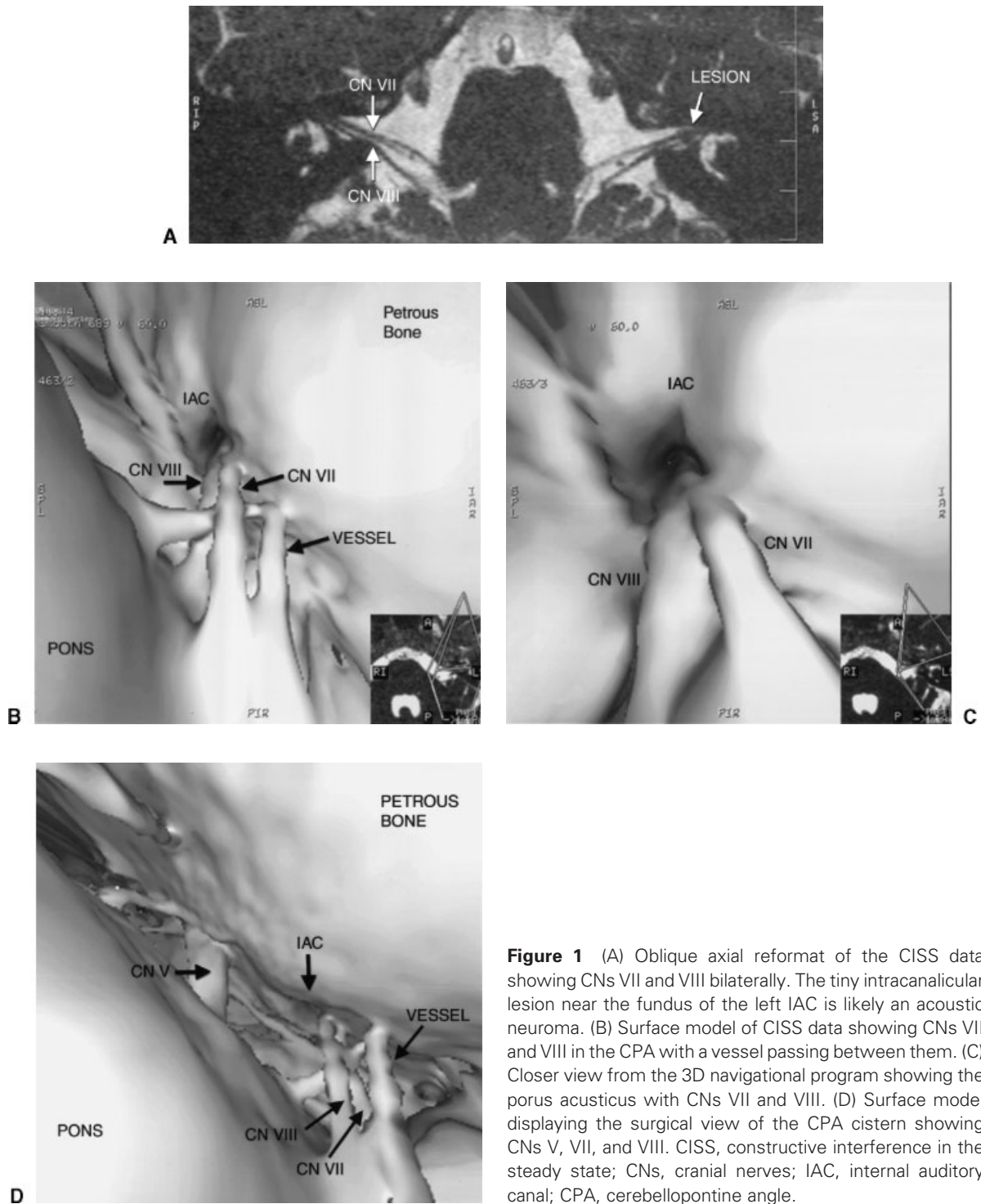


**Figure 1** (A) Oblique axial reformat of the CISS data showing CNs VII and VIII bilaterally. The tiny intracanalicular lesion near the fundus of the left IAC is likely an acoustic neuroma. (B) Surface model of CISS data showing CNs VII and VIII in the CPA with a vessel passing between them. (C) Closer view from the 3D navigational program showing the porus acusticus with CNs VII and VIII. (D) Surface model displaying the surgical view of the CPA cistern showing CNs V, VII, and VIII. CISS, constructive interference in the steady state; CNs, cranial nerves; IAC, internal auditory canal; CPA, cerebellopontine angle.

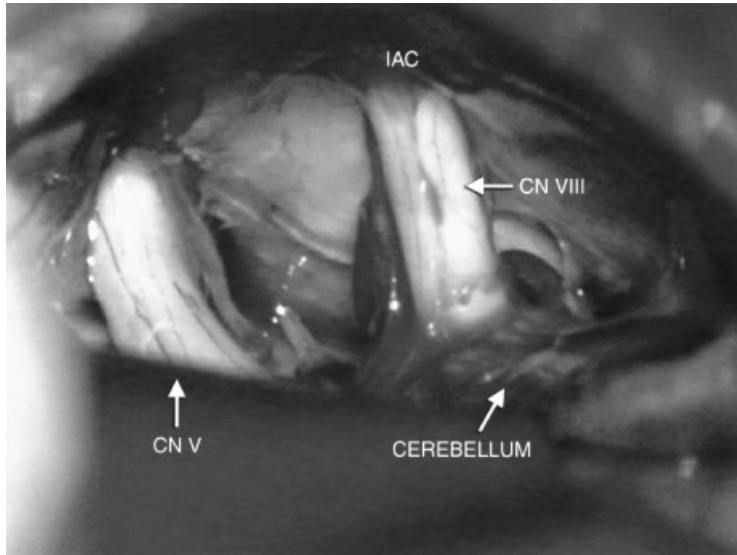


**Figure 2** Intraoperative image of the CPA cistern from the suboccipital approach showing CNs V, VII, and VIII. CPA, cerebellopontine angle; CNs, cranial nerves.

intraoperative photography through the operating microscope confirmed the anatomic accuracy of the 3D models (Fig. 2). The method is limited for lesions deep in the IAC where surfaces are too small to resolve. The relationship between the CNs and acoustic neuromas can be evaluated (Fig. 3). Figure 4 shows a chondrosarcoma arising from the

petroclival synchondrosis adjacent to CNs V, VII, and VIII. Vascular structures that are often seen in relation to CNs VII and VIII can be viewed in a 3D format to aid evaluation of and surgical planning for microvascular decompression. Figure 5 shows how vascular loops can contact CN VII or VIII in the CPA cistern.

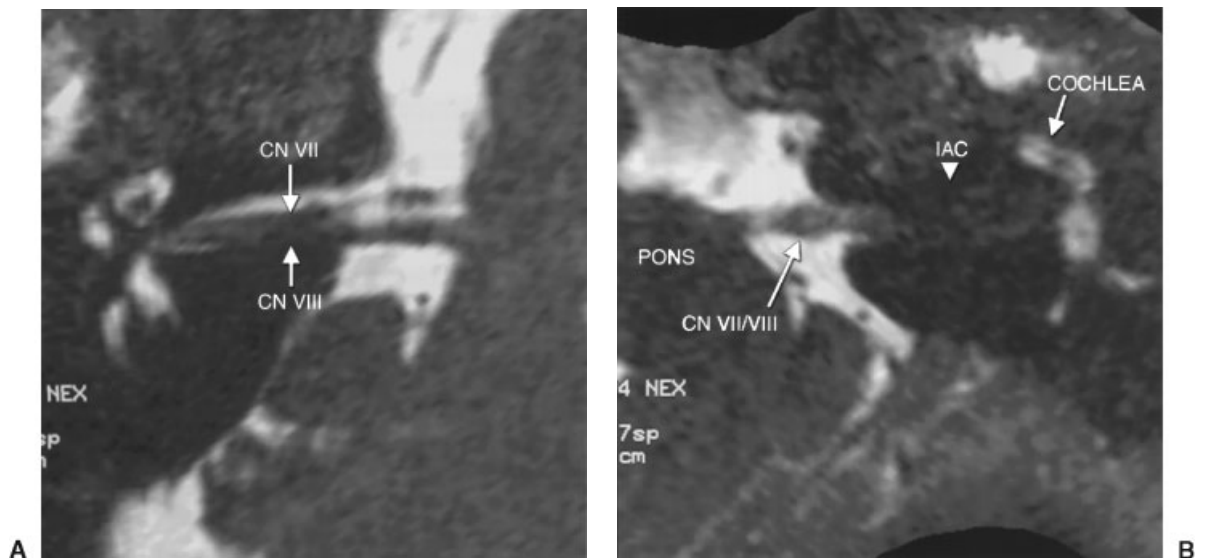


**Figure 3** (A) Oblique axial reformat of CISS data shows the right IAC with CNs VII and VIII. (B) Oblique axial reformat of CISS data shows the left CPA with the acoustic neuroma filling the IAC.

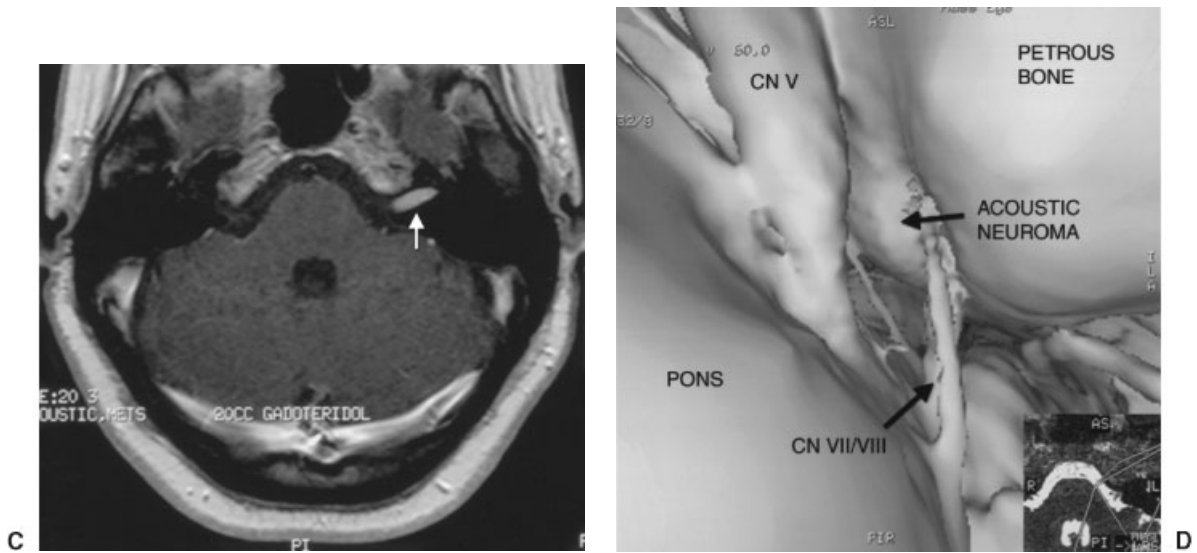


**Figure 3** (continued) (C) Axial T1-weighted postgadolinium image shows an enhancing lesion in the left IAC consistent with an acoustic neuroma. (D) Surface-rendered model of the left petrous face shows the acoustic neuroma filling the IAC as CNs VII and VIII enter the canal. CISS, constructive interference in the steady state; IAC, internal auditory canal; CNs, cranial nerves; CPA, cerebellopontine angle.

**DISCUSSION**

Imaging used to create an interactive neurosurgical planning tool must demonstrate a high degree of anatomic detail. Virtual cisternscopy uses a

surface-rendered model generated from CISS data, which has 3D anatomic detail similar to that seen during neurosurgical approaches to the CPA cistern. CISS data demonstrate the root entry zones and the cisternal and intracanalicular portions of

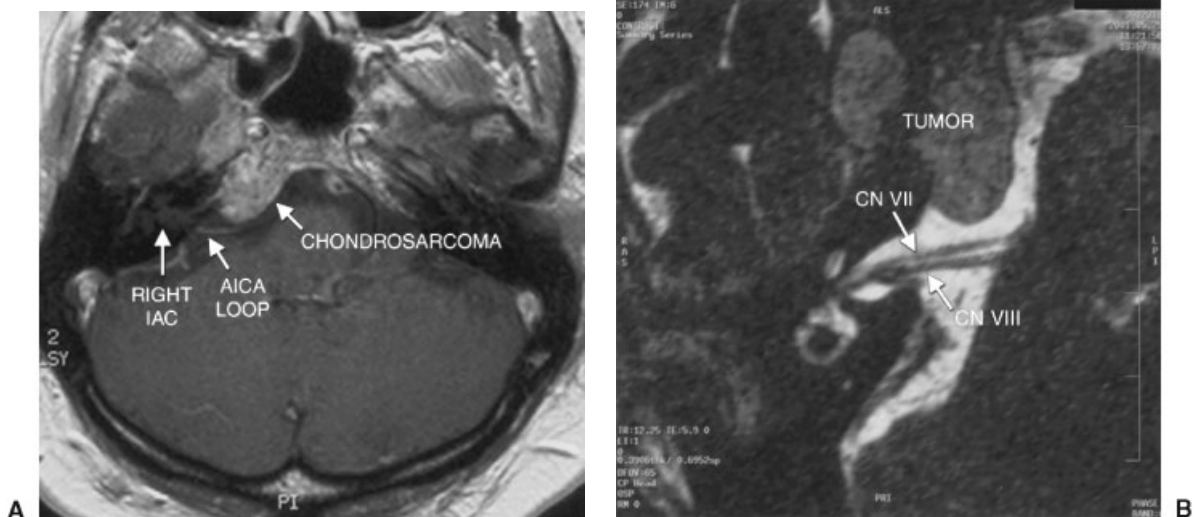


**Figure 4** (A) Postgadolinium T1-weighted axial image shows the right skull base chondrosarcoma projecting into the CPA cistern. The right IAC appears normal with a small vessel seen as the enhancing linear structure near the canal. (B) Oblique reformat of CISS data shows CNs VII and VIII in the right CPA and IAC. AICA, anterior inferior cerebellar artery.

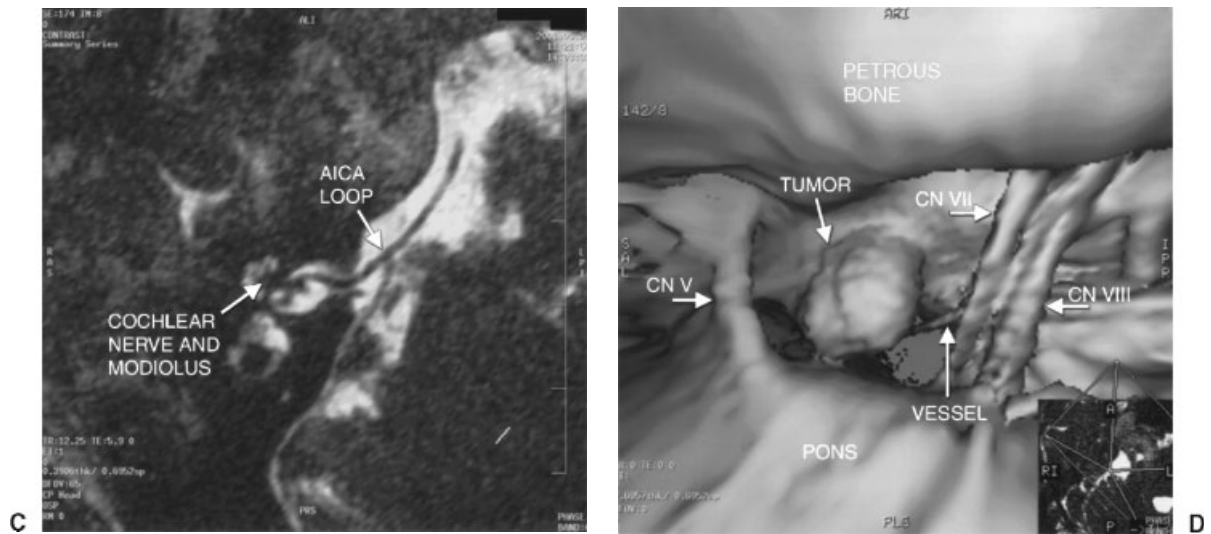


**Figure 4** (continued) (C) Oblique reformat of CISS data shows a vessel anterior to the right IAC. (D) Surface-rendered model from the navigational model shows the tumor near CNs VII and VIII. The vessel is also identified near the IAC. CPA, cerebellopontine angle; IAC, internal auditory canal; CISS, constructive interference in the steady state; CNs, cranial nerves.

each nerve with high detail. The 2D and axial source data should be included in the evaluation of a study to confirm the findings made with this 3D technique.

The neurosurgical approach is done with the patient in a supine position on the operating table with the head turned parallel to the floor. The suboccipital exposure allows the surgeon to visualize

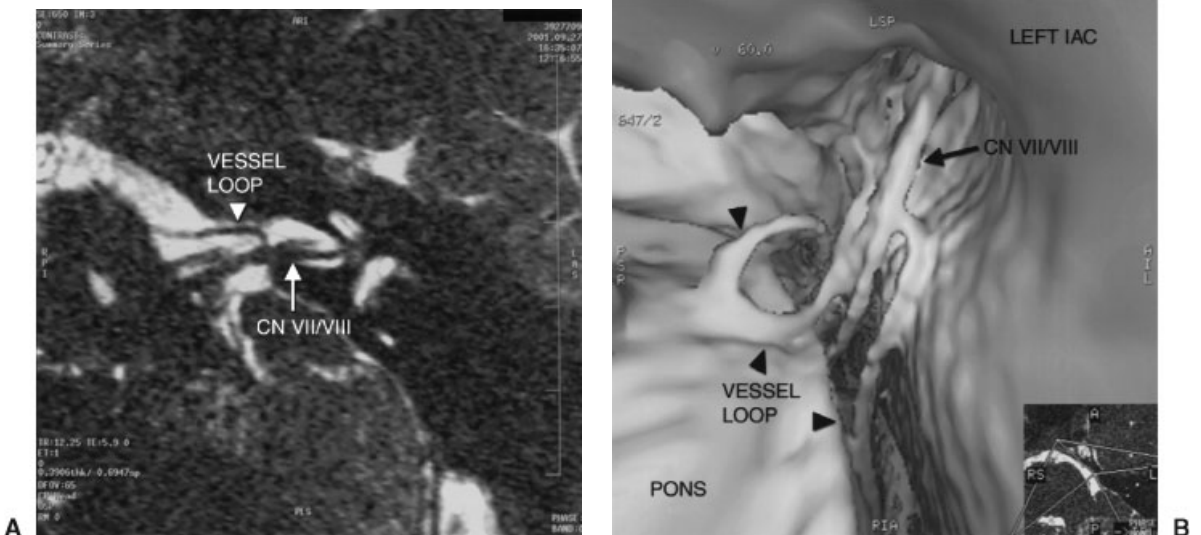


**Figure 5** (A) Oblique axial reformat of CISS data shows a vessel loop, a branch of the anterior inferior cerebellar artery, near CNs VII and VIII at the porus acusticus. (B) Surface model of the left IAC shows the prominent vessel loop in contact with CNs VII and VIII. Vessel loops at this location or at the root entry zone on the brain stem can cause hemifacial spasm. CISS, constructive interference in the steady state; CNs, cranial nerves; IAC, internal auditory canal.

the posterior petrous face once the cerebellum is retracted.<sup>7</sup> Images created by our method can be viewed from this perspective as well as from any other point in the CSF space. The interactive mode provides information for surgical planning.

Surface-rendered images show distortion of near objects at the periphery of the visual field. This distortion is similar to the effect of a macrolens. Consequently, the data must be evaluated with the 2D reformats, the axial raw data, and routine images. Artifacts related to CSF motion, particularly from pulsation around the basilar artery, and skull base susceptibility can compromise the datasets and 3D models. Other MRI pulse sequences that may show less artifact such as 3D-FASE (3D fast asymmetric spin echo)<sup>8</sup> and SIMCAST (segmented-interleaved motion-compensated acquisition in the steady state)<sup>9</sup> also could be used in this postprocessing method.

## REFERENCES

1. Casselman JW, Kuhweide R, Deimling M, Ampe W, Dehaene I, Meeus L. Constructive interference in the steady state-3DFT MR imaging of the inner ear and cerebellopontine angle. *AJNR Am J Neuroradiol* 1993;14:47-57
2. Naganawa S, Koshikawa T, Fukatsu H, Ishigaki T, Fukuta T. MR Cisternography of the cerebellopontine angle: comparison of three-dimensional fast asymmetrical spin-echo and three dimensional constructive interference in the steady state sequences. *AJNR Am J Neuroradiol* 2001;22:1179-1185
3. Shigematsu Y, Korogi Y, Hirai T, et al. Virtual MRI endoscopy of the intracranial cerebrospinal fluid spaces. *Neuroradiology* 1998;40:644-650
4. Boor S, Maurer J, Mann W, et al. Virtual endoscopy of the inner ear and the auditory canal. *Neuroradiology* 2000;42:543-547
5. Diamantopoulos II, Ludman CN, Martel AL, et al. Magnetic resonance imaging virtual endoscopy of the labyrinth. *Am J Otol* 1999;20:748-751
6. Heine C, Klingebiel R, Lehman R. Three-dimensional MR visualization of the intracisternal course of the cranial nerves V-VIII by virtual cisternography. *Acta Radiol* 2002;43:242-248
7. Ojemann RG. Retrosigmoid approach to acoustic neuroma (vestibular schwannoma). *Neurosurgery* 2001;48:553-559
8. Yang D, Kodama T, Tamura S, Watanabe K. Evaluation of the inner ear by 3D fast asymmetric spin echo (FASE) MR imaging: phantom and volunteer studies. *Magn Reson Imaging* 1999;17:171-182
9. Kurucay S, Schmalbrock P, Chakeres DW, Keller PJ. A segmented-interleaved motion-compensated acquisition in the steady state (SIMCAST) technique for high-resolution imaging of the inner ear. *J Magn Reson Imaging* 1997;7:1060-1068

## Commentary

The authors present a novel magnetic resonance imaging technique for visualizing structures of the cerebellopontine angle from any perspective. When treating vascular compression syndromes, this technique would be especially useful to define precisely the relationship of vascular structures to the associated cranial nerves. Its utility in preoperative planning for skull base tumors is self-evident. This technique would be a welcome addition to any skull base practice.

Randall W. Porter, M.D.<sup>1</sup>